Geol. Mag. **143** (*4*), *2006, pp. 431–446.* © *2006 Cambridge University Press*
doi:10.1017/S0016756806001968 *Printed in the United Kingdom*

Geology and timing of dextral strike-slip shear zones in Danmarkshavn, North-East Greenland Caledonides

C. SARTINI-RIDEOUT*†, J. A. GILOTTI* & W. C. McCLELLAND‡

*Department of Geoscience, University of Iowa, Iowa City, IA 52240, USA
‡Department of Geological Sciences, University of Idaho, Moscow, ID 83844, USA

(*Received* 28 April 2005; *accepted* 18 October 2005)

Abstract – The North-East Greenland eclogite province is divided into a western, central and eastern block by the sinistral Storstrømmen shear zone in the west and the dextral Germania Land deformation zone in the east. A family of steep, NNW-striking dextral mylonite zones in the Danmarkshavn area are geometrically and kinematically similar to the ductile Germania Land deformation zone, located 25 km to the east. Amphibolite facies deformation at Danmarkshavn is characterized by boudinage of eclogite bodies within quartzofeldspathic host gneisses, pegmatite emplacement into the boudin necks and subsequent deformation of pegmatites parallel to gneissosity, a widespread component of dextral shear within the gneisses, and localization of strain into 10–50 m thick dextral mylonite zones. The gneisses and concordant mylonite zones are cut by a swarm of weakly to undeformed, steeply dipping, E–W-striking pegmatitic dykes. Oscillatory-zoned zircon cores from two boudin neck pegmatites give weighted mean $^{206}Pb/^{238}U$ sensitive, high mass resolution ion microprobe (SHRIMP) ages of 376 ± 5 Ma and 343 ± 7 Ma. Cathodoluminescence images of these zircons reveal complex additional rims, with ages from ranging from *c*. 360 to 320 Ma. Oscillatory-zoned, prismatic zircons from two late, cross-cutting pegmatites yield weighted mean $^{206}Pb/^{238}U$ SHRIMP ages of 343 ± 5 Ma and 332 ± 3 Ma. Zircons from the boudin neck pegmatites record a prolonged growth history, marked by fluid influx, during amphibolite facies metamorphism beginning at *c*. 375 Ma. The cross-cutting pegmatites show that dextral deformation in the gneisses and ductile mylonite zones had stopped by *c*. 340 Ma. Ultrahigh-pressure metamorphism in the eastern block at 360 Ma requires that the Greenland Caledonides were in an overall contractional plate tectonic regime. This, combined with 20 % steep amphibolite facies lineations in the eclogites, gneisses and mylonites suggests that dextral transpression may have been responsible for a first stage of eclogite exhumation between 370 and 340 Ma.

Keywords: eclogite, exhumation, Greenland Caledonides, U–Pb SHRIMP geochronology, zircon.

1. Introduction

Subduction of continental material to high- and ultrahigh-pressure (UHP) conditions in collisional settings is well documented (Ernst & Liou, 2000; Chopin, 2003; Massone & O'Brien, 2003; Shatsky & Sobolev, 2003). Processes by which these rocks were exhumed are not as well understood. Extension during convergence has been the favoured mechanism for exhumation of regional high-pressure terranes, whether by underplating and consequent extension during convergence (Platt, 1986), by extensional collapse triggered by removal of the lithospheric roots (Dewey, 1988; Andersen *et al.* 1991), or buoyancy-driven uplift of the subducted crustal slice triggered by erosion (Beaumont, Fullsack & Hamilton, 1994; Chemenda *et al.* 1995; Chemenda, Mattauer & Bokun, 1996). Alternatively, strike-slip shear zones can accommodate exhumation (Fossen & Tikoff, 1998) in both transpressional settings (Mann & Gordon, 1996; Thompson, Schulmann & Jezek, 1997*a*, *b*; Lin, Jiang & Williams, 1998; Jiang, Lin & Williams, 2001) and transtensional settings (Krabbendam & Dewey, 1988; Avé Lallemant, 1996).

The North-East Greenland eclogite province (NEGEP) (Fig. 1a) represents a portion of the Laurentian margin that was subjected to high-pressure and ultrahigh-pressure conditions during the Caledonian orogeny. The province is divided into three structural blocks by two major strike-slip faults: the sinistral Storstrømmen shear zone (SSZ) and the dextral Germania Land deformation zone (GLDZ). The other prominent tectonic feature in the eclogite province is the Norreland thrust in the western block (Hull, Gilotti & Friderichsen, 1995; Jepsen, 2000). The Storstrømmen shear zone has been proposed as a regionally significant strike-slip shear zone which accommodated, together with the foreland thrusts in Dronning Louise Land, sinistral transpression in North-East Greenland in the Silurian and early Devonian (Holdsworth & Strachan, 1991; Dewey & Strachan, 2003). The significance of the Germania Land deformation zone in this model, or in exhumation of the eclogite province in general, has not been addressed.

† Author for correspondence: claudia-sartini@uiowa.edu

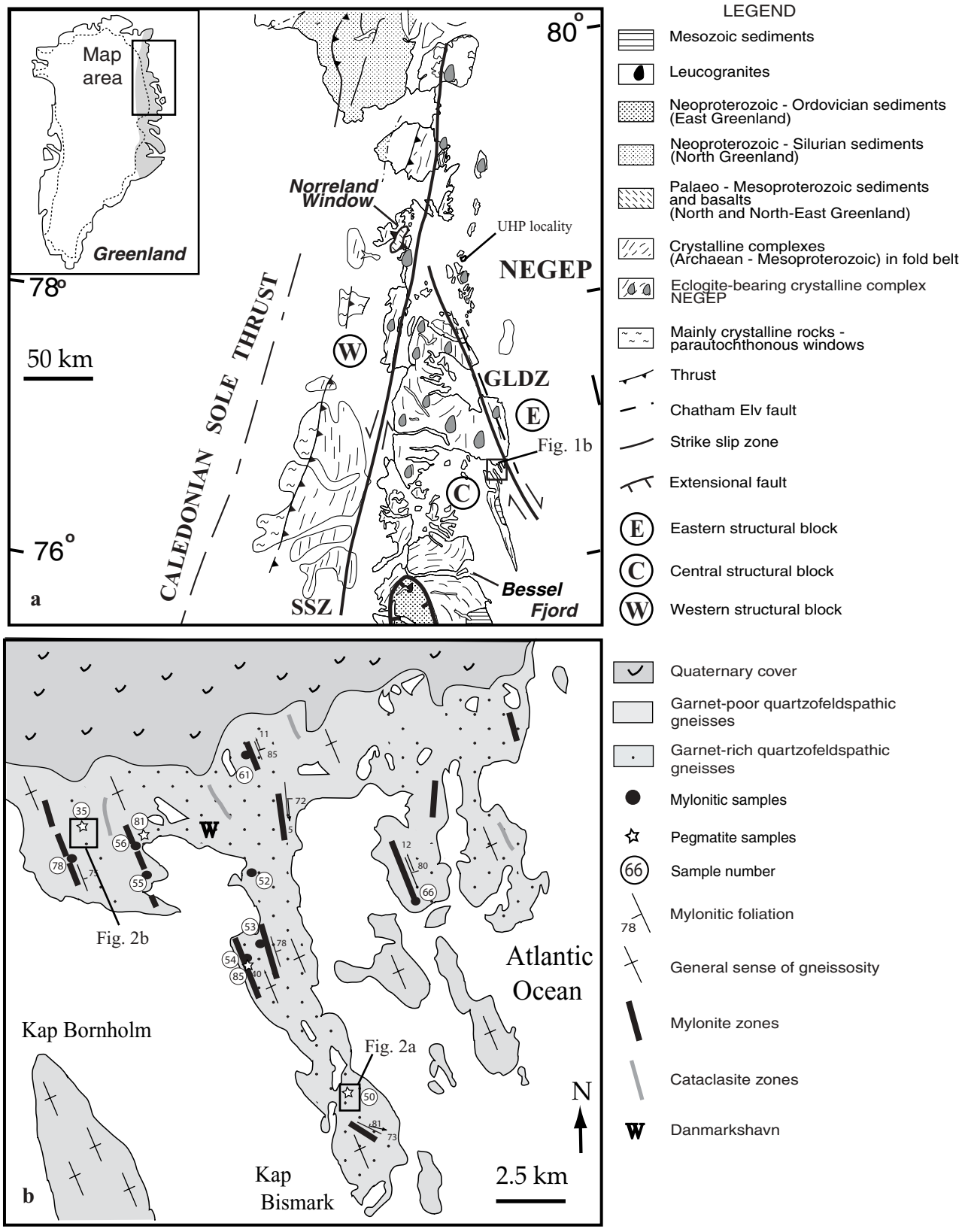

Figure 1. (a) Geological map showing the North-East Greenland eclogite province (NEGEP) and the major tectonic features: Storstrømmen shear zone (SSZ) and the Germania Land deformation zone (GLDZ), after Henriksen (2003). (b) Geological map of the Danmarkshavn area. Locations are shown for samples mentioned in text.

Recent geochronology in the eclogite province yielded ages of 410–390 Ma for HP metamorphism in the western and central blocks, and 360 Ma for UHP in the eastern block (Gilotti, Nutman & Brueckner, 2004). The ages imply that activity along the Storstrømmen shear zone is post-390 Ma, and some movement along the Germania Land deformation zone is post-360 Ma, because both shear zones overprinted the eclogites at lower pressures. This paper focuses on providing additional bounds on the timing of the Germania Land deformation zone in order to determine its role in exhumation of UHP (ultrahigh-pressure) and HP (high-pressure) rocks in the central and eastern blocks. We report observations on a series of smaller-scale dextral mylonite zones in the Danmarkshavn area, which is located just west of the Germania Land deformation zone (Fig. 1). The physical conditions of mylonite formation, kinematics, and timing of the Danmarkshavn shear zones are interpreted as representing the earliest stages of movement on the larger Germania Land deformation zone. We present U–Pb zircon geochronology from pegmatites that cross-cut the mylonite zones at Danmarkshavn, and hence limit the age of motion along individual shear zones. Finally we discuss the possible role of transpression along the Germania Land deformation zone in the exhumation of the North-East Greenland eclogite province.

2. Regional geology

The North-East Greenland eclogite province (Gilotti, 1993) represents the uppermost thrust sheet in the stack of sheets that forms the northeastern portion of the Laurentian margin. Local internal imbrication is present in the gneiss complex, especially south of 76° N (Chadwick & Friend, 1994); it is more difficult to recognize in the north (Hull *et al.* 1994). The eclogite province (Fig. 1a) consists of amphibolite facies orthogneisses derived from 2.0 to 1.8 Ga calc-alkaline intrusive complexes and 1.74 Ga granitic intrusions overprinted by Caledonian metamorphism (Kalsbeek, Nutman & Taylor, 1993; Hull *et al.* 1994; Kalsbeek, 1995; Brueckner, Gilotti & Nutman, 1998). The quartzofeldspathic orthogneisses contain metre-scale mafic pods with variably preserved eclogite facies assemblages. The pods are flattened into lenses parallel to the gneissosity of the surrounding host rocks. The eclogite facies rocks include eclogites *sensu stricto,* garnet websterites, garnet clinopyroxenites, coronitic gabbroic intrusions and websterites (Gilotti, 1994). Protoliths of the eclogite facies rocks were pre-Caledonian mafic dykes, mafic to ultramafic intrusions and mafic xenoliths in the calc-alkaline batholiths (Gilotti, 1993, 1994; Brueckner, Gilotti & Nutman, 1998).

The protoliths of the gneisses and mafic rocks are the same in the three structural blocks, however, the age and pressure–temperature (*P–T*) conditions of the metamorphism vary. The western and central blocks (Fig. 1a) were metamorphosed under medium-*T* (600–750 °C), high-*P* (1.5–2.3 GPa) conditions (Brueckner, Gilotti & Nutman, 1998; Elvevold & Gilotti, 2000) in the Devonian, with the age of HP metamorphism varying between 410 and 390 Ma (Gilotti, Nutman & Brueckner, 2004). Parts of the eastern block (Fig. 1a), on the other hand, experienced ultrahigh-pressure metamorphism. Coesite is included in zircons from eclogites as well as the host gneisses (Power *et al.* 2004). Thermobarometry on the peak assemblage garnet + omphacite + kyanite + phengite + coesite gives temperatures above 950 °C at 3.6 GPa (Gilotti & Ravna, 2002). The UHP metamorphism is 360 Ma or younger based on a $^{206}U/^{238}Pb$ ages from coesite-bearing metamorphic zircon in kyanite eclogite (Gilotti, Nutman & Brueckner, 2004; McClelland *et al.* 2005).

The Storstrømmen shear zone (SSZ) was first described as a 10 km wide, 1000 km long, sinistral, strike-slip ductile shear zone (Holdsworth & Strachan, 1991). The mylonites may be as thick as 1 km (Hull & Gilotti, 1994). The Storstrømmen shear zone is discontinuous along its length, segmented into *en echelon* zones (see Jepsen, 2000). The steep mylonites strike NNE and contain gently SSW-plunging lineations (Strachan & Tribe, 1994). The mylonites are thought to have formed at lower amphibolite facies conditions, based on the texturally stable matrix assemblage of hornblende–K-feldspar–biotite–quartz and subgrain formation in feldspar porphyroclasts, which suggest temperatures greater than 450 °C (Strachan & Tribe, 1994; Hallett *et al.* 2005). The ductile mylonitic fabric is overprinted by quasiplastic deformation. Both ductile and semi-ductile deformation zones are locally cut by narrow cataclastic bands (Strachan & Tribe, 1994). The presence of 350 Ma titanite porphyroclasts in the mylonites suggest that the Storstrømmen shear zone was active after this time (Hallett *et al.* 2005).

The Germania Land deformation zone (GLDZ) includes two subparallel high-strain zones separated by approximately 2 km, which strike between 335 and 345° (Hull & Gilotti, 1994), and can be traced for *c*. 100 km along strike. The width of individual shear zones varies between 10 m and a few hundred metres. Gneissosity and the mylonitic foliation are subparallel and vertical. Mylonitic lineations are dominantly quartz and feldspar aggregate stretching lineations that plunge shallowly to the NNW, although some have a down-dip orientation. A dextral sense of shear can be deduced from numerous micro- and mesoscale kinematic indicators. Preliminary work on the Germania Land deformation zone shows that deformation occurred predominantly under greenschist facies conditions, as evident from the matrix assemblage of quartz + K-feldspar + biotite ± plagioclase ± epidote ± chlorite, and the absence of recrystallized amphibole (Hull & Gilotti, 1994). An earlier history of activity at amphibolite facies cannot be ruled out, which is compatible with

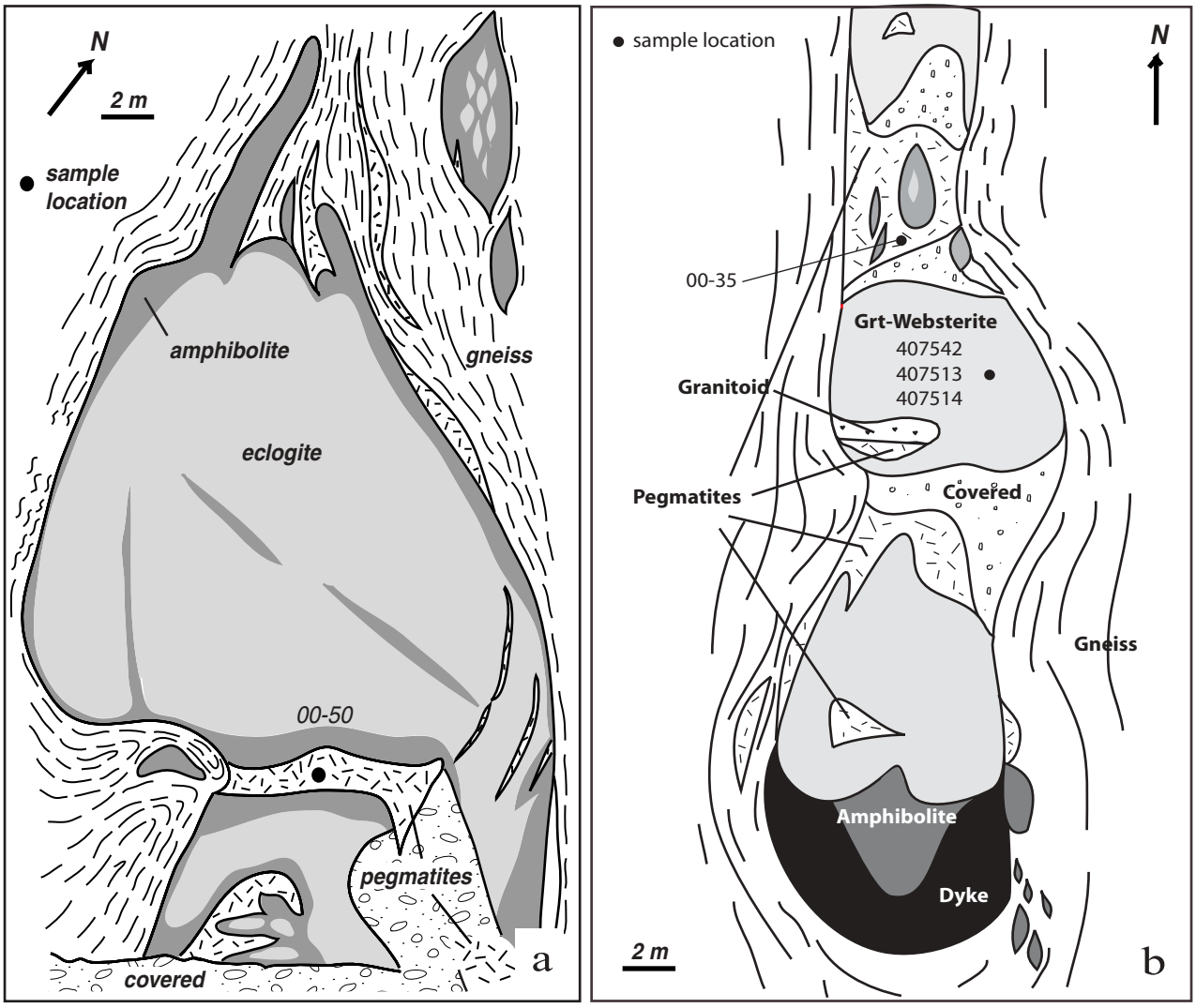

Figure 2. Detailed outcrop maps of HP (high-pressure) mafic pods surrounded by quartzofeldspathic orthogneisses. (a) A boudinaged eclogite with pronounced amphioblite facies rims. Pegmatites occur in boudin necks, in curved fractures within the eclogite and on the margin of the body. Note U–Pb sample 00-50. (b) A boudinaged, massive garnet websterite body with pegmatites in boudin necks and along the pod margins. Sample 00-35 used for U–Pb dating.

the metamorphic grade of the surrounding gneisses. The deformation zone is also locally overprinted by cataclasites consisting of chlorite + quartz + calcite + sericite. A 100 m thick brittle normal fault zone, the Chatham Elv fault, was mapped at the eastern margin of the Germania Land deformation zone (Hull & Gilotti, 1994). The magnitude of displacement along the two major strike-slip shear zones is a matter of debate. While Holdsworth & Strachan (1991) propose displacements along the Storstrømmen shear zone of tens to hundreds of kilometres, Hull & Gilotti (1994) estimate the displacement to be an order of magnitude less, largely based on the absence of observed offset lithologies. The newly recognized difference in age of metamorphism and *P–T* conditions between the eastern and the central blocks (Gilotti & Ravna, 2002; Gilotti, Nutman & Brueckner, 2004) suggests that significant displacement could have occurred along the Germania Land deformation zone. This raises the question of the possible role played by this structure in the exhumation of the high-pressure terranes in North-East Greenland.

3. Geology of the Danmarkshavn area

The Danmarkshavn area (76°46′ N, 18°40′ W) is situated about 25 km west of the Germania Land deformation zone, in the southeastern part of the eclogite province (Fig. 1a, b). The area was chosen for detailed study because some background geology and geochronology exists (Henriksen, 1997), and the field relationships between the eclogites, host gneisses, mylonites and pegmatites are particularly well exposed (e.g. Fig. 2a, b). In addition, the small-scale shear zones

at Danmarkshavn are geometrically and kinematically similar to the larger Germania Land deformation zone (Hull & Gilotti, 1994), and they are cut by a swarm of pegmatites that provide limits on movement of the dextral shear zones. The main geological features of the Danmarkshavn area are described below.

3.a. Host gneisses

Gneisses in the Danmarkshavn area are similar to the Precambrian quartzofeldspathic gneisses that host eclogites throughout the North-East Greenland eclogite province. They are dominated by quartzofeldspathic orthogneisses derived from the calc-alkaline batholiths, with less abundant paragneiss. An enclave of Archaean gneiss has been recognized (Steiger *et al.* 1976; Nutman & Kalsbeek, 1994) within the dominantly Palaeoproterozoic gneisses. The two cannot be distinguished on the basis of field evidence, but we interpret the Archaean gneiss as a block of wall rock to the 2.0–1.8 Ga calc-alkaline intrusions. The gneisses contain alternating layers of lighter coloured, more felsic material, with and without garnet, intercalated with screens of darker, more garnetiferous paragneisses. The layers are on the order of a few hundred metres to a kilometre wide. The orthogneisses are composed of garnet + hornblende + feldspar + quartz + biotite ± clinopyroxene (Fig. 3a). The paragneisses consist of garnet + feldspar + sillimanite + hornblende + epidote + biotite + quartz (Fig. 3b). The orthogneisses are the main protolith of the mylonites.

Several metagranitoid bodies (10–30 m wide, 50–100 m long) are also present in the gneiss complex. Although the metagranites have not been dated in Danmarkshavn, they most likely correlate with the 1.74 Ga granitoid suite dated by Kalsbeek, Nutman & Taylor (1993) and described by Hull *et al*. (1994). These lens-shaped bodies are concordant with the gneissosity and contain a relatively simple Caledonian foliation that is parallel to the polyphase gneissosity.

The gneissosity is isoclinally folded but consistently strikes between 340 and 350° and has a sub-vertical dip (Fig. 4). The planar fabric is defined by the preferred orientation of amphibole laths and compositional layering. Object lineations (Piazolo & Passchier, 2002) defined by stretched feldspar and by hornblende grains are also present. The lineations trend approximately 350°, but vary between shallowly (5–15°) to steeply plunging (Fig. 4). Clear, overprinting relationships between the horizontal and vertical lineations cannot be discerned by field relations; the two lineations may in part be coeval.

3.b. Eclogites

The plethora of eclogite facies rocks documented around Danmarkshavn (Gilotti, 1993, 1994; Brueckner, Gilotti & Nutman, 1998) substantiates Bronner's (1948) initial field observations of 'bright green eclogite' and Wyllie's (1957) recognition of a 'bronzitite' near the weather station. The eclogitic pods are typically one metre to several hundred metres long, and are found primarily as oblate ellipsoids within both the orthogneisses and the paragneisses. They can be a single lithology or compositionally layered, with kyanite eclogite, bimineralic eclogite (garnet and omphacite) and garnet websterite all occurring together in the same pod. Detailed maps of a typical boudinaged eclogite pod and a garnet websterite layer are shown in Figure 2. Two generations of mafic dykes are recognized in the Danmarkshavn gneisses (Deutmeyer *et al.* 2001). The older dykes are concordant with the gneisses and commonly boudinaged, while the second generation clearly cross-cuts the gneisses and metagranitoids. They are both fine- to medium-grained amphibole + plagioclase ± garnet ± clinopyroxene assemblages. Many contain coronitic and symplectitic textures indicative of partial eclogitization and retrogression from eclogite facies, respectively. All of the dykes were strongly deformed in the Caledonian.

The textures of the eclogitic pods vary from massive and undeformed to strongly deformed L-S and L tectonites. Compositional layering, when present, is commonly isoclinally folded. Object lineations are defined by the high-pressure minerals garnet, clinopyroxene and kyanite, and by retrograde minerals including stretched feldspars and amphibole. The plunge of the lineation is consistently steep to subvertical (Fig. 4). In one outcrop, both eclogite facies and retrograde mineral lineations are present in a single layered body, and are sub-parallel. The margins of most pods are retrogressed and deformed in the amphibolite facies, with a foliation concordant to the surrounding amphibolite facies host gneisses (e.g. Fig. 2a).

Brueckner, Gilotti & Nutman (1998) determined the *P–T* conditions and age of the eclogite facies metamorphism at Danmarkshavn from the medium-grained, massive garnet websterite shown in Figure 2b. These rocks were selected because the lower variance assemblage, garnet + orthopyroxene + clinopyroxene, is more amenable to thermobarometry than the simple garnet + omphacite eclogites. Brey & Kohler's (1990) thermometer and barometer yields a peak *P* of 2.35 GPa at 790 °C for sample 407513. A Sm–Nd garnet + orthopyroxene + clinopyroxene + amphibole + whole rock mineral isochron for the same garnet websterite (sample 407542) is 370 ± 12 Ma, younger than the 410–390 Ma estimate for HP metamorphism of the central block (Gilotti, Nutman & Brueckner, 2004). U–Pb SHRIMP ages of zircon from the centre of the eclogite pod and its amphibolite facies margin (Fig. 2a) fall in the range 380–370 Ma (McClelland & Gilotti, 2003), which is interpreted as the age of retrograde amphibolite facies metamorphism. Thus the Sm–Nd isochron age may record retrograde metamorphism rather than the age of peak *P*.

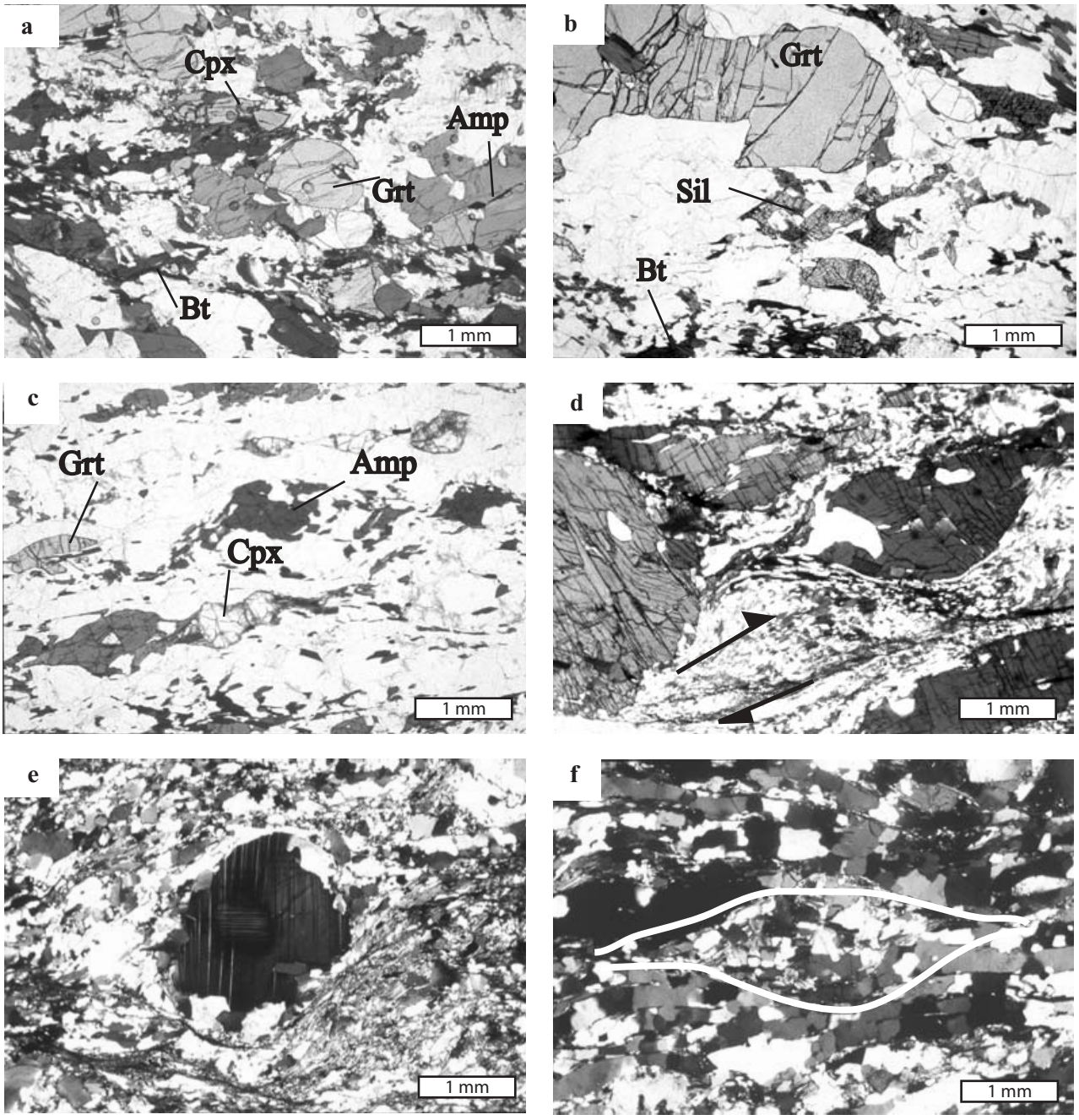

Figure 3. Photomicrographs of protolith gneisses and mylonites. All photos at the same scale. See Table 1 for mineral abbreviations. (a) Typical orthogneiss contains garnet, amphibole, biotite, clinopyroxene, plagioclase and quartz. Gneissosity is defined by compositional layering and preferred orientation of biotite and in some cases amphibole. (b) A paragneiss composed of garnet, sillimanite, amphibole, biotite, feldspar and quartz. (c) Protomylonite with porphyroclasts of garnet, clinopyroxene and amphibole. (d) Two generations of amphibole are present as porphyroclasts and matrix grains in this mylonite. The recrystallized hornblende forms shear bands, indicating dextral shear during amphibolite facies conditions. (e) K-feldspar porphyroclast with core and mantle texture. (f) A completely recrystallized feldspar porphyroclast surrounded by quartz ribbons consisting of polygonized strain-free grains that indicate static recrystallization and recovery.

3.c. Mylonite and cataclasite zones

Mylonites and spatially and temporally unrelated cataclasites form high-strain zones in the gneisses around Danmarkshavn (Figs 1b, 5a). The mylonitic shear zones are several centimetres to 5–6 m thick and over 200 m long, oriented approximately parallel to the gneissosity (Fig. 4). They are marked by pronounced grain size reduction and the formation of augen.

Sixteen mylonite and protomylonite samples were examined with the petrographic microscope to establish their mineralogy, microstructure and the physical conditions of deformation (Table 1). The overall consistent mineralogy is quartz + feldspar + garnet ±

Table 1. Mineralogy and microstructures of representative gneisses and mylonites from the Danmarkshavn area

Sample	Rock type	Grt	Amp	Cpx	Bt	Sil	Fsp	Qtz	Chl	Ep	Sph
00-9	Orthogneiss	pc	pc	pc	m		pc/m	m		pc	a
407511	Mylonite	pc	m				pc/m	pc/m	f		pc
00-13	Mylonite	pc	pc		m		pc/m	m/f/r	f		
407518	Mylonite	pc			m		pc/m	m/r	f		
00-18	Orthogneiss	pc			n		pc/m	m/m-new	n		
00-19	Orthogneiss	pc			n		pc/m	m/m-new	n		
00-21	Paragneiss	pc	pc/m-new		n/m-new	pc	pc/m/m-new	m/m-new		pc	
00-43	Orthogneiss	pc	pc/m-new	pc	m-new		m-new/m	m-new/m		pc	a
00-52	Mylonite		pc/m-new	pc	m-new		pc/m	m-new/r			
00-53	Myloite	pc/neo	m-new	pc	m-new		pc/m-new	m-new/r			
00-54	Mylonite	pc/neo	pc		m-new		pc/m	m-new/r			
00-55	Mylonite	pc			m-new		pc/m-new	m-new/r			
00-56	Mylonite	pc			m-new		pc/m-new	m-new/r			
00-61	Mylonite	pc	pc/m-new	pc	m-new		m-new	m-new/r			
00-66	Mylonite	pc			n/m-new		pc/m-new	m-new/r			
00-78	Mylonite		m-new		m-new		m-new	m-new			

pc – porphyroclast; n – neoblast; m-new – neoblastic mineral in matrix; m – matrix; r – ribbons; a – accessory; f – filling fractures; Grt – garnet; Amp – amphibole; Cpx – clinopyroxene; Bt – biotite; Sil – sillimanite; Fsp – feldspar; Qtz – quartz; Chl – chlorite; Ep – epidote; Sph – sphene.

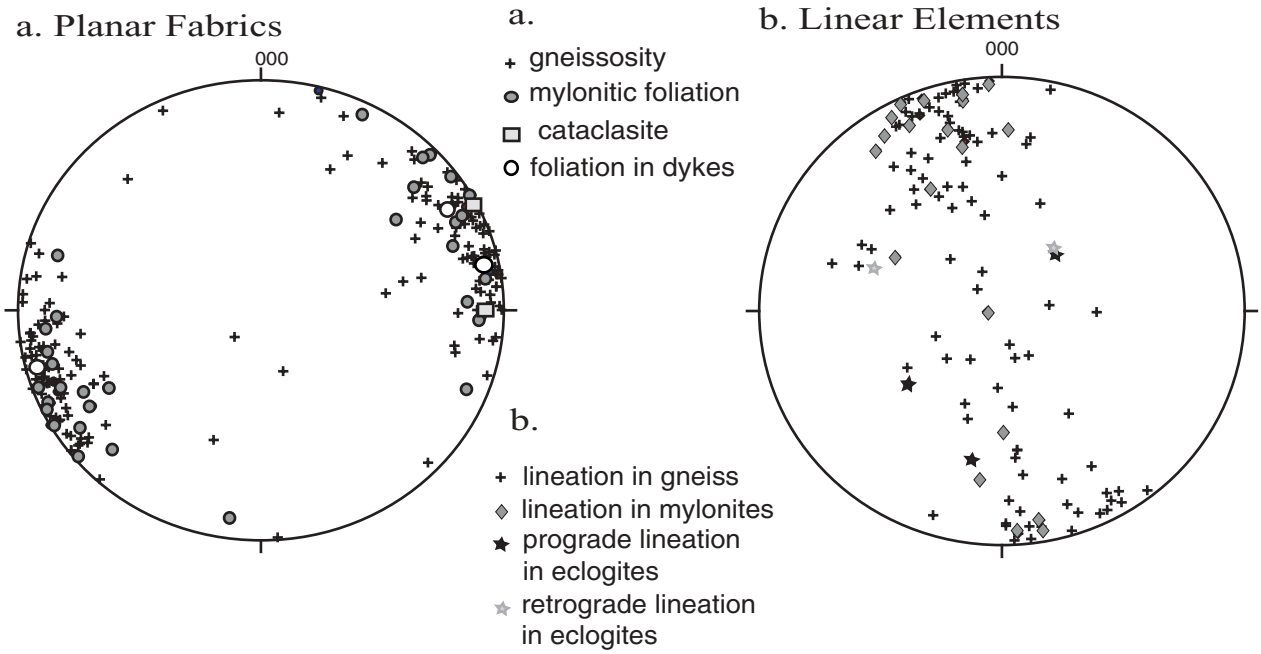

Figure 4. Lower hemisphere stereographic projections of (a) planar and (b) linear elements in the gneisses, eclogites and mylonites.

clinopyroxene ± hornblende + biotite ± chlorite (Fig. 3c). In addition to the finely recrystallized quartz and feldspar, biotite and hornblende were also formed during shearing as can be deduced by the preferred orientation of these minerals and their occurrence in shear bands (Fig. 3d). Chlorite partially replaces biotite in some of the mylonites.

Quartz ribbons are very common in these rocks. Quartz grains in the ribbons and recrystallized grains in the matrix are strain-free. Static recrystallization with rapid recrystallization and recovery is recognized in the strain-free grains, and in the elongated crystals in the ribbons which might indicate grain boundary area reduction (Fig. 3e). Grain boundary migration recrystallization can be recognized, especially around feldspar porphyroclasts. Feldspar core and mantle textures are present in a continuum with complete replacement of porphyroclasts by subgrains (Fig. 3e, f), indicating the transition between subgrain rotation recrystallization and grain boundary migration recrystallization deformation (Vidal *et al.* 1980; Tullis & Yund, 1985, 1991; Stipp *et al.* 2002).

The mylonitic foliation is defined by a preferred orientation of planar minerals and is subparallel to the steeply dipping gneissosity. Object lineations are mostly defined by stretched feldspar porphyroclasts, but some amphibole object lineations are also present. Aggregate lineations are defined by dynamically recrystallized feldspar grains. Both types of lineations lie in the mylonitic foliation and generally plunge 5–15°

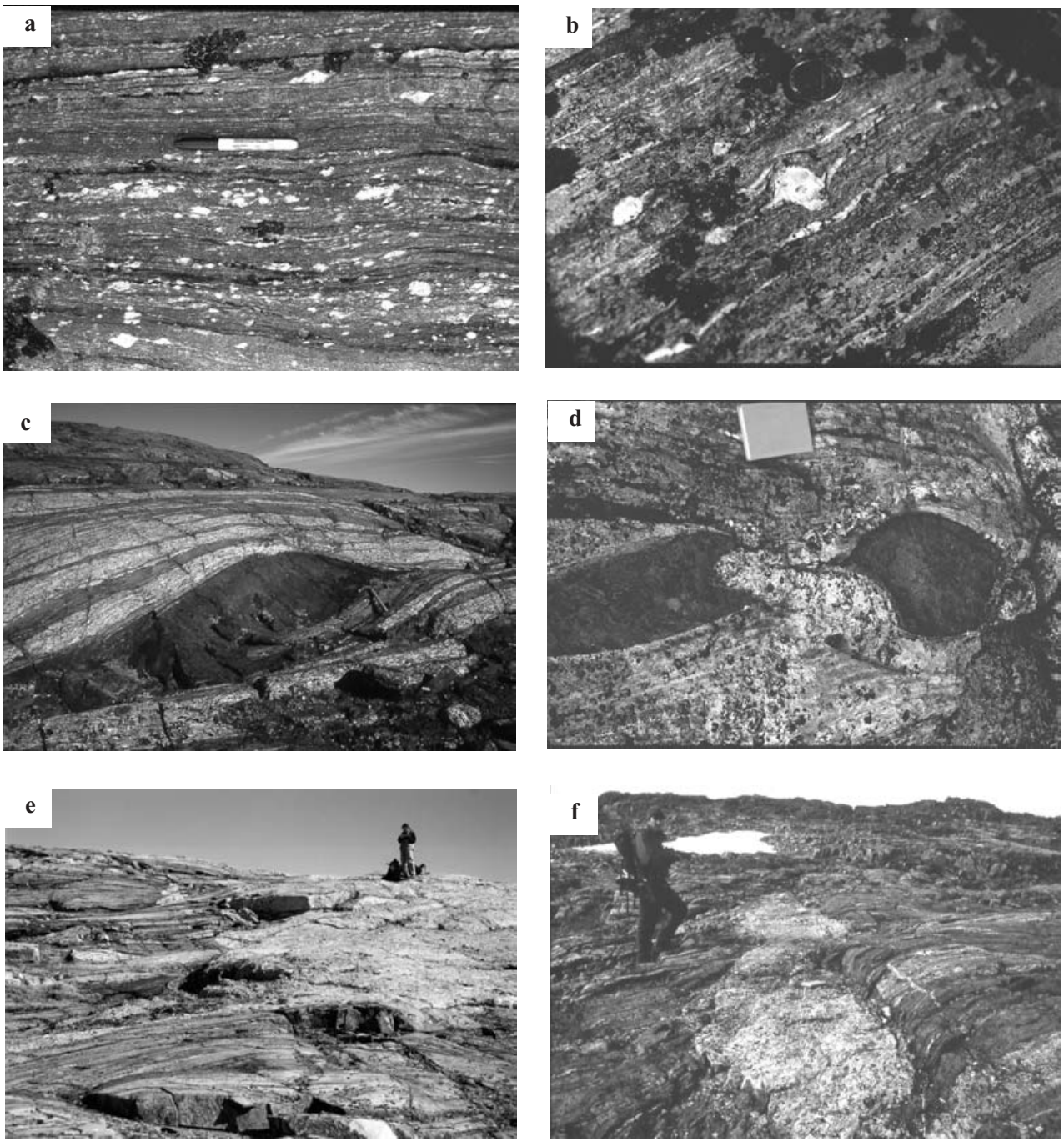

Figure 5. (a) Mylonite with abundant σ-porphyroclasts indicating a dextral shear sense. Marker is 13 cm long. (b) Dextral δ-porphyroclast of a pegmatite stringer in a typical augen mylonite. Coin diameter is 2.5 cm. (c) A sigmoidal shaped mafic pod surrounded by grey, mylonitized orthogneiss and a deformed, isoclinally folded pegmatite gives a dextral sense of shear. Hammer is 40 cm long. (d) Boudinaged mafic pod with a pegmatite filling the boudin neck. Length of notebook is 19 cm. (e) Pegmatite cross-cutting gneisses and a mylonite zone at high angle (location of sample 00-85). The relationship of the foliation to the margin of the pegmatitic body varies along its edges. The gneissosity is undisturbed by the pegmatite, while the mylonitic foliation is deflected into flanking structures. Person for scale. (f) White pegmatite cross-cuts gneisses and a shear zone (black rocks in foreground) at a high angle. The gneissosity and the mylonitic foliation are deflected adjacent to the pegmatite. Person for scale.

to the N (Fig. 4). The shear zones are dominated by the sub-horizontal component, however, *c.* 20 % of the measured lineations, including both those defined by feldspar (object and aggregate) and amphibole, plunge up to 74° (Fig. 4). There is no clear timing relationship between the horizontal and vertical lineations. Since both are formed by minerals grown at amphibolite facies, we conclude that they may be broadly synchronous.

Kinematic indicators in the mylonite zones consistently give a dextral sense of shear. At the mesoscale, σ- and δ-feldspar porphyroclasts are abundant (Fig. 5b); in

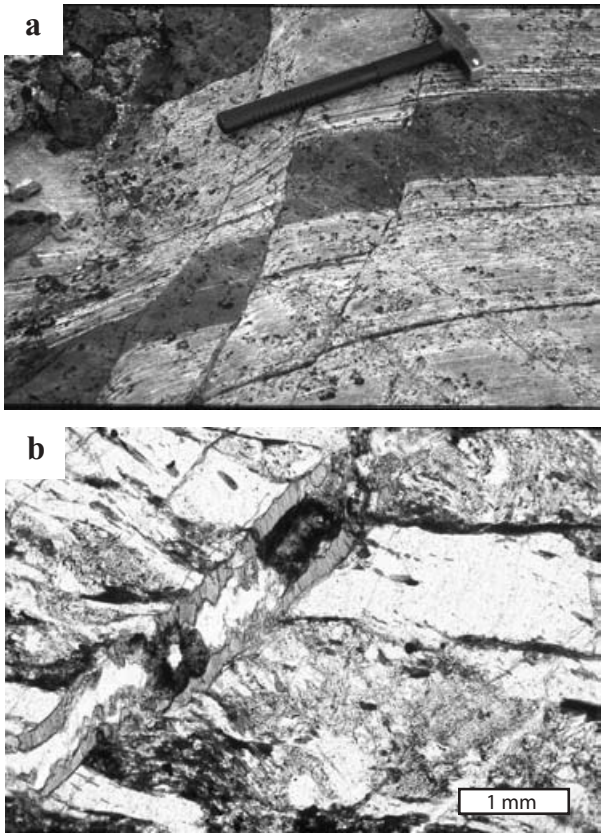

Figure 6. Examples of brittle deformation. (a) Domino displacement of a mafic dyke along brittle fractures. Hammer is 40 cm long. (b) A microcrack filled by chlorite and microcrystalline quartz.

addition, some of the mafic pods in the highly deformed gneisses are asymmetric and sigmoidal in shape (Fig. 5c). The right lateral shear sense is confirmed by numerous microscopic σ- and δ-shaped porphyroclasts. The majority of the asymmetric porphyroclasts are feldspar (Fig. 3e, f), but hornblende forms sigma structures as well. Quartz ribbons are often microfolded but the fold asymmetries do not consistently indicate a specific sense of shear. Shear bands, marked by a preferred orientation of recrystallized amphibole and biotite (Fig. 3d) in discrete zones, corroborate the dextral shear sense.

Brittle deformation is widespread throughout the Danmarkshavn area as discrete zones. Four prominent cataclasite zones were mapped (Fig. 1b). These brittle deformation zones are a few metres to tens of metres wide and 10–100 m long, with the same orientation as the mylonite zones (Fig. 4). They are typically composed of coarse, heterogeneous breccias and are green in colour. Unlike the Chatham Elv fault, no fault gouge is observed. Domino displacement of some of the mafic dykes occurs along discrete brittle fractures (Fig. 6a). Microscopic observations reveal that the brittle deformation also overprints the mylonites. Transgranular fractures in the mylonites, filled with chlorite and/or finely recrystallized quartz, cut across porphyroclasts, quartz ribbons and matrix (Fig. 6b).

3.d. Pegmatites

Granitic pegmatites are abundant in the Danmarkshavn area. Three main types of pegmatites are recognized: NNW–SSE bodies within mylonitic zones, pegmatites in the necks of mafic boudins (Figs 2, 5d), and E–W-striking tabular bodies that cross-cut the gneisses and mylonite zones at high angles (Fig. 5e, f).

The NNW–striking pegmatites, coplanar with the gneissic foliation and shear zones, are strongly deformed by the same shear that generated the mylonites. These pegmatites are commonly isoclinally folded (Fig. 5c), with the axial plane of the isoclinal folds parallel to the mylonitic foliation. Lenticular K-feldspar grains up to 5 cm long are common, many with a σ-shape, indicating dextral sense of shear.

The pegmatites in the boudin necks are spatially associated with the retrogressed margins of the eclogitic pods, and thus taken to be the syn-deformational melts emplaced during amphibolite facies metamorphism. The boudin neck pegmatites rarely have grains greater than 1 cm in diameter and are undeformed except at the margins of the bodies. Similar pegmatites fill fractures within pods (e.g. Fig. 2c).

The swarm of cross-cutting granitic pegmatites defined by E–W lenticular bodies is similar in size and orientation to numerous swarms recognized along the east coast of Stormlandet, Germania Land and Store Koldewey (Henriksen, 1997). Individual pegmatite bodies vary from 5 to 100 m long and 1 to 30 m wide. Grain size is generally coarser than in the boudin neck pegmatites, with plagioclase grains up to 5 cm across. Some of the cross-cutting pegmatites are deformed both at the mesoscale and at the microscale, with a weak E–W foliation parallel to the contacts of the pegmatites. The foliation is defined by orientation of the planar mafic minerals and flattened feldspar grains. Thin-section observation reveals ϕ-shape porphyroclasts of plagioclase and K-feldspar accompanied by moderate recrystallization and grain-size reduction of quartz and feldspar grains. Quartz ribbons are present. Most of the recrystallized quartz grains have undulose extinction, and the grain boundaries vary from polygonal to almost interlobate. The weak deformation in the pegmatites has no asymmetry and is geometrically unrelated to the mylonites and the gneisses. There is no evidence of a second E–W foliation superimposed on the mylonites or gneisses adjacent to the pegmatites. The gneissosity and the mylonitic foliation are commonly deflected to form flanking folds (Passchier, 2001) in the proximity of the deformed pegmatitic bodies (Fig. 5f). Other cross-cutting E–W pegmatites are undeformed and have irregular boundaries (Fig. 5e).

4. Pegmatite geochronology

Zircons from two boudin neck pegmatites, samples 00-35 and 00-50 (Fig. 2) and two cross-cutting pegmatites, samples 00-81 and 00-85 (Fig. 1b), were dated in order to bracket the time of displacement on the ductile mylonite zones.

4.a. Sample description

Sample 00-35 was collected from the boudin neck of a stretched garnet websterite pod (Fig. 2b). The pegmatite consists of approximately 45 % plagioclase, 30 % quartz, 10 % K-feldspar, 10 % biotite and 5 % chlorite + muscovite. The sample is undeformed both at the outcrop scale and microscopically. It presents an inequigranular, interlobate fabric, and shows evidence of grain boundary migration recrystallization of quartz.

Sample 00-50 was collected from the boudin neck of an eclogite *sensu stricto* (Fig. 2a). This sample consists of 40 % plagioclase, 30 % quartz, 10 % K-feldspar, 15 % biotite, and 5 % chlorite + muscovite. It is also undeformed, and presents the same inequigranular, interlobate fabric and evidence for grain boundary migration recrystallization of quartz grains as 00-35.

Sample 00-81 was collected from a 20 m long by 5 m wide pegmatite cross-cutting a mylonite zone (Fig. 1b). It consists of approximately 50 % K-feldspar, 25 % plagioclase, 10 % quartz, 10 % biotite and 5 % epidote, Fe-rich zoisite, chlorite and muscovite. The sample is weakly deformed with ϕ-shape porphyroclasts of plagioclase and K-feldspar accompanied by recrystallization and grain-size reduction of quartz and feldspar grains.

Sample 00-85 was also collected from a pegmatite cross-cutting a mylonite zone (Figs 1b, 5e). The pegmatitic body, 100 m long by 30 m wide, is one of the largest in the area. The sample, composed of 60 % K-feldspar, 20 % plagioclase, 15 % quartz, 5 % biotite + chlorite + muscovite, is also deformed and is texturally similar to sample 00-81.

4.b. U–Pb SHRIMP methods

Zircon was separated from each of the four 1–3 kg pegmatite samples and analysed for U–Pb on the SHRIMP-RG (sensitive high mass resolution ion microprobe – reverse geometry) instrument at the United States Geological Survey–Stanford University Ion Probe Laboratory, Stanford, CA, USA. Once concentrated by standard gravimetric and magnetic techniques, grains for analysis were hand-picked under alcohol on the basis of clarity, lack of inclusions and integrity. Selected grains were mounted in epoxy and polished to expose grain centres. Cathodoluminesence (CL) images were used to characterize the zircons and select spots for analysis. Calibration concentrations of U and Th were based on analyses of zircon standard SL13. Isotopic compositions were calibrated by replicate analyses of zircon standard R33 (419 Ma). The analytical routine followed Williams (1997) and Barth, Wooden & Coleman (2001). Data reduction and plotting utilized programs of Ludwig (1999, 2001). U–Pb data for each sample discussed below are plotted on a Tera-Wasserburg diagram (Fig. 7) and presented in Table 2. Uncertainties in the isotopic ratios are reported at the 1σ level. Ages are assigned based on the weighted mean of observed $^{206}Pb/^{238}U$ ages corrected using the ^{207}Pb correction method. Weighted mean age uncertainties are reported at the 95 % confidence level.

4.c. U–Pb SHRIMP results

Boudin neck sample 00-35 has euhedral zircons characterized by cores with broad to fine oscillatory growth zoning overprinted by domains with more complex growth zoning and resorption textures (Fig. 8a). Most grains have well-developed higher U rims. The cores have $^{206}Pb/^{238}U$ ages ranging from 347 to 388 Ma, U concentrations of 105–690 ppm, and Th/U ratios of 0.03–0.05 with two additional low ratios of 0.002–0.003. Eight of the 14 core analyses give a weighted mean $^{206}Pb/^{238}U$ age of 376 ± 5 Ma with a mean square of weighted deviate (MSWD) = 1.2. Analyses from the distinct high U rims (U = 765–1609 ppm) yield a weighted mean $^{206}Pb/^{238}U$ age of 339 ± 4 Ma (MSWD = 0.7). The remaining six core analyses were taken in oscillatory-zoned domains characterized by complex growth zoning and resorption near core–rim boundaries (Fig. 8a). Four of these analyses yield a weighted mean $^{206}Pb/^{238}U$ age of 361 ± 3 Ma (MSWD = 0.5) that may represent an additional growth period. Alternatively, the intermediate ages may represent recrystallization or Pb loss within 376 Ma zircon core domains during rim growth at approximately 340 Ma.

Zircons from the second boudin neck sample, 00-50, are euhedral and characterized by broad to fine oscillatory-zoned cores (Fig. 8b). Rare xenocrystic cores are present. The inner core domain is overprinted by outer areas of fine oscillatory-zoned to unzoned zircon formed in areas of growth and resorption, respectively. Both of the core regions are overgrown by higher U rims. Ages obtained from the inner core domain range from 491 to 339 Ma with U concentrations of 175–405 ppm and Th/U ratios of 0.05–0.07. The oldest age likely results from analysis of a mixture of xenocrystic core and new pegmatite zircon. Excluding this spot, the remaining analyses give a weighted mean $^{206}Pb/^{238}U$ age of 343 ± 7 Ma (MSWD = 3.0). Zircon in the outer core domain has slightly higher U concentrations of 280–950 ppm and yields a weighted mean $^{206}Pb/^{238}U$ age of 327 ± 3 Ma (MSWD = 1.1). The distinct rims, which are high U (640–2040 ppm) and low Th/U (0.02–0.05), give a weighted mean $^{206}Pb/^{238}U$ age of 317 ± 2 Ma (MSWD = 0.7).

Samples of cross-cutting pegmatites contain euhedral broad to fine oscillatory-zoned zircons that in CL

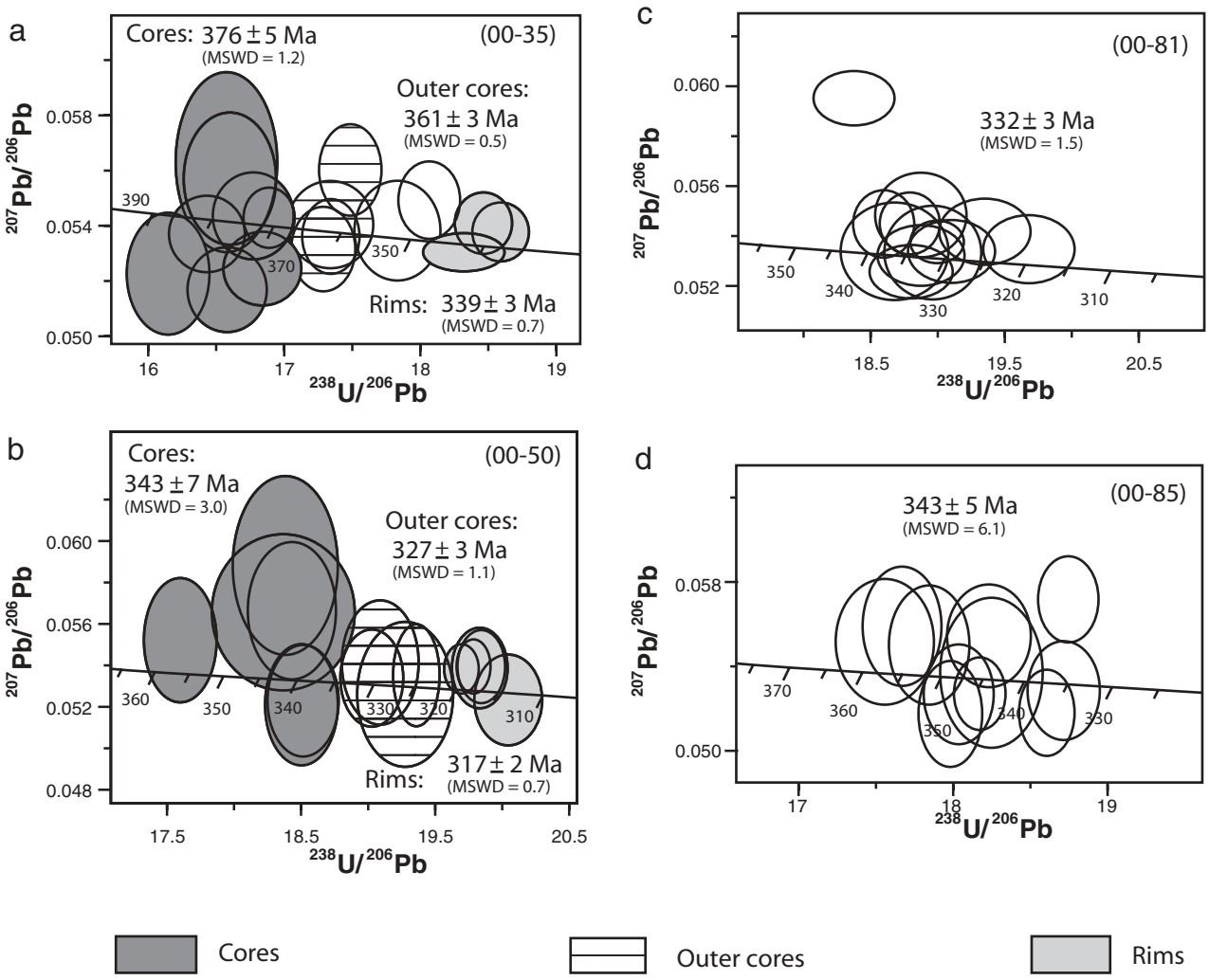

Figure 7. Tera-Wasserburg plots for dated pegmatites. Data uncorrected for common Pb are plotted with error ellipses at the 1σ level. (a) Sample 00-35. Analyses used for calculation of weighted mean $^{206}Pb/^{238}U$ ages (2σ) for differing CL domains observed in boudin neck pegmatite samples (a) 00-35 and (b) 00-50 are denoted by dark grey-filled ellipses for homogeneous core regions, horizontal ruled ellipses for intermediate rims, and light grey for distinct rims. Calculated weighted mean $^{206}Pb/^{238}U$ ages (2σ) for cross-cutting pegmatite samples (c) 00-81 and (d) 00-85 utilized all plotted analyses. MSWD = mean square of weighted deviates.

images appear uniform in sample 00-81 (Fig. 8c), and show a slight core to rim variation in U concentration in sample 00-85 (Fig. 8d). Narrow higher U rims that were too thin for analysis are present on some zircons from sample 00-85 as well. Sample 00-81 gave a weighted mean $^{206}Pb/^{238}U$ age of 332 ± 3 Ma (MSWD = 1.5). Ages from sample 00-85 are more variable, ranging from 333 to 356 Ma and yielding a weighted mean $^{206}Pb/^{238}U$ age of 343 ± 5 Ma (MSWD = 6.1). Although the observed scatter may be attributed to multiple growth events similar to those observed in the boudin neck pegmatites, there is not a well-defined correlation between compositional or textural domain and age.

The zircon data presented above indicate that the Danmarkshavn area experienced multiple periods of pegmatite emplacement, both in the necks of boudins and as cross-cutting bodies. In addition, the boudin neck pegmatites record a protracted zircon growth history. On the basis of the relatively low Th/U ratios, all of the zircons are interpreted to have formed from metamorphic fluids, most likely associated with retrograde amphibolite facies metamorphism. The zircon core age for sample 00-35 demonstrates that emplacement of boudin neck pegmatites was ongoing by 375 Ma. Crystallization of additional zircon is attributed to fluid influx during continued retrograde metamorphism and deformation at approximately 340 and perhaps 360 Ma. Zircon rim growth in sample 00-35 at 340 Ma was synchronous with emplacement of additional boudin neck material at locality 00-50 and cross-cutting pegmatite 00-85. Similarly, additional zircon crystallization in sample 00-50 was accompanied by pegmatite emplacement at locality 00-81 at approximately 330 Ma.

The boudin neck pegmatites record a protracted history of zircon crystallization that can be attributed to repeated influx of metamorphic fluid into this

Table 2. U–Pb SHRIMP geochronological data and apparent ages

Spot[a]		U[b] (ppm)	Th (ppm)	Th/U	$^{206}Pb^{*b}$ (ppm)	$f^{206}Pbc^{b}$	$^{238}U/^{206}Pb_c$	$^{207}Pb/^{206}Pb_c$	$^{206}Pb/^{238}U^{d}$ (Ma)
Sample 00-35: pegmatite in boudin neck (UTM 27 0556500; 8522700)									
1.1	c	376	15	0.04	20	0.06	16.44 (1.2)	0.0537 (1.8)	380.8 (4.4)
2.1	r	1609	8	0.005	75	0.03	18.32 (1.1)	0.0530 (0.9)	342.7 (3.6)
3.1	c	482	20	0.04	24	0.19	16.84 (1.2)	0.0525 (1.6)	372.5 (4.2)
4.1	c	230	9	0.04	12	0.03	16.16 (1.3)	0.0523 (2.8)	388.1 (4.9)
5.1	c2	392	14	0.04	19	0.04	17.34 (1.2)	0.0541 (1.9)	361.3 (4.3)
6.1	c	164	8	0.05	8	0.20	16.61 (1.4)	0.0557 (2.8)	376.2 (5.1)
7.1	c2	528	24	0.05	25	0.04	17.84 (1.2)	0.0538 (2.3)	351.4 (4.1)
8.1	c	104	0.2	0.002	5	0.28	16.57 (1.5)	0.0563 (3.8)	376.7 (5.6)
9.1	c	313	10	0.03	16	0.30	16.57 (1.2)	0.0517 (2.0)	378.8 (4.5)
10.1	c	326	12	0.04	17	0.04	16.78 (1.2)	0.0544 (1.9)	373.0 (4.4)
11.1	c2	501	19	0.04	25	0.02	17.35 (0.8)	0.0536 (1.7)	361.4 (3.0)
12.1	c2	398	13	0.03	20	0.08	17.29 (0.9)	0.0532 (2.0)	362.7 (3.2)
13.1	c2	537	21	0.04	26	0.19	18.07 (0.8)	0.0549 (1.7)	346.7 (2.9)
14.1	c2	415	1	0.003	20	0.29	17.48 (0.9)	0.0560 (2.0)	357.6 (3.2)
15.1	c	691	27	0.04	35	0.03	16.90 (0.8)	0.0543 (1.4)	370.4 (2.8)
16.1	r	765	9	0.01	36	0.10	18.46 (0.8)	0.0541 (1.4)	339.7 (2.6)
17.1	r	867	10	0.01	40	0.07	18.59 (0.8)	0.0538 (1.3)	337.5 (2.5)
Sample 00-50: pegmatite in boudin neck (UTM 27 0562700; 8515900)									
1.1	r	642	14	0.02	28	0.01	20.05 (0.8)	0.0523 (2.9)	314 (3)
2.1	r	2035	34	0.02	89	0.13	19.71 (0.4)	0.0538 (1.6)	319 (1)
2.2	c	350	17	0.05	17	0.20	17.60 (1.0)	0.0553 (3.6)	356 (4)
3.1	c	373	19	0.05	17	0.01	18.50 (1.0)	0.0521 (3.7)	340 (3)
4.1	c	176	8	0.05	8	0.69	18.39 (1.4)	0.0588 (4.9)	339 (5)
4.2	r	1051	22	0.02	46	0.14	19.83 (0.7)	0.0539 (2.4)	317 (2)
5.1	c	405	27	0.07	19	0.01	18.51 (1.0)	0.0523 (3.5)	340 (3)
5.2	r	1049	23	0.02	45	0.15	19.84 (0.7)	0.0539 (2.2)	317 (2)
6.1	c	194	9	0.05	9	0.41	18.38 (1.9)	0.0565 (4.4)	340 (6)
6.2	c2	949	22	0.02	42	0.07	19.37 (0.6)	0.0535 (3.1)	324 (2)
7.1	c2	495	31	0.06	22	0.05	19.03 (0.8)	0.0534 (2.9)	330 (3)
7.2	r	1705	39	0.02	74	0.15	19.78 (0.5)	0.0539 (1.6)	317 (1)
8.1	c2	281	21	0.08	13	0.01	19.28 (1.2)	0.0526 (4.3)	326 (4)
9.1	c2	397	22	0.06	18	0.13	19.08 (1.0)	0.0541 (3.7)	329 (3)
9.2	c	271	15	0.06	13	0.42	18.43 (1.2)	0.0566 (3.9)	339 (4)
10.1	c	347	21	0.06	24	2.85	12.27 (1.9)	0.0801 (2.3)	491 (9)
10.2	r	1995	96	0.05	79	0.94	21.63 (0.5)	0.0596 (2.8)	289 (2)
Sample 00-81: cross-cutting pegmatite (UTM 27 0558000; 8521900)									
1.1	c	607	26	0.04	27	0.04	19.10 (1.1)	0.0534 (1.5)	329 (4)
2.1	c	885	56	0.07	41	0.78	18.36 (1.1)	0.0595 (1.2)	339 (4)
3.1	c	247	9	0.04	11	0.02	18.67 (1.4)	0.0534 (2.4)	336 (5)
4.1	c	276	11	0.04	13	0.03	18.96 (1.3)	0.0533 (2.3)	331 (4)
5.1	c	876	46	0.05	40	0.01	18.80 (1.1)	0.0525 (1.3)	334 (4)
6.1	c	374	16	0.04	17	0.21	18.86 (1.2)	0.0548 (2.1)	332 (4)
7.1	c	683	31	0.05	30	0.16	19.34 (1.2)	0.0542 (1.6)	324 (4)
8.1	c	687	31	0.05	30	0.08	19.68 (1.2)	0.0534 (1.7)	319 (4)
9.1	c	735	35	0.05	33	0.01	18.87 (1.1)	0.0532 (1.5)	333 (4)
10.1	c	639	33	0.05	29	0.17	18.78 (0.8)	0.0545 (1.5)	334 (3)
11.1	c	1458	120	0.08	66	0.09	18.99 (0.7)	0.0538 (1.1)	331 (2)
12.1	c	579	31	0.06	27	0.15	18.59 (0.8)	0.0544 (1.7)	337 (3)
Sample 00-85: cross-cutting pegmatite (UTM 27 0560500; 8519200)									
1.1	r	319	22	0.07	15	0.05	18.25 (1.2)	0.0537 (4.4)	344 (4)
1.2	c	494	30	0.06	24	0.19	17.85 (1.0)	0.0550 (3.4)	351 (3)
2.1	r	395	22	0.06	19	0.19	17.56 (1.2)	0.0552 (3.6)	356 (4)
2.2	c	770	55	0.07	37	0.01	17.98 (0.8)	0.0518 (3.2)	350 (3)
3.1	r	1177	84	0.07	56	0.08	18.17 (0.6)	0.0527 (2.2)	346 (2)
3.2	c	647	46	0.07	31	0.29	17.67 (1.0)	0.0559 (3.4)	354 (3)
4.1	c	978	97	0.10	45	0.01	18.61 (0.6)	0.0518 (2.6)	338 (2)
5.1	c	597	33	0.06	27	0.01	18.72 (0.8)	0.0529 (3.0)	336 (3)
6.1	c	162	8	0.05	8	5.58	17.82 (1.6)	0.0980 (8.8)	333 (6)
7.1	c	627	42	0.07	30	0.01	18.04 (0.8)	0.0527 (3.0)	348 (3)
8.1	c	604	40	0.07	28	0.27	18.23 (1.0)	0.0555 (2.9)	343 (3)
9.1	c	806	62	0.08	37	0.51	18.75 (0.7)	0.0572 (2.4)	333 (2)

Note: All analyses were performed on the SHRIMP-RG ion microprobe at the Stanford–United States Geological Survey Microanalytical Center at Stanford University. Calibration concentrations and isotopic compositions were based on replicate analyses of SL13 and R33
(419 Ma), respectively. Analytical routine followed Williams (1997). Data reduction utilized Ludwig (2001).

[a]Abbreviations: c = core; c2 = second core domain observed in CL images; r = rim.

[b]Pb^{*} denotes radiogenic Pb; Pb_c denotes common Pb; $f^{206}Pb_c = 100*(^{206}Pb_c/^{206}Pb_{total})$.

[c]Reported ratios are not corrected for common Pb. Errors are reported in parentheses as percent at the 1σ level.

[d]Ages calculated from ratios corrected for common Pb using ^{207}Pb for the $^{206}Pb/^{238}U$ age. Uncertainties in millions of years reported as 1σ. Ages in bold were used in calculation of weighted mean $^{206}Pb/^{238}U$ ages for core domains. Ages in italics were used in calculation of weighted mean $^{206}Pb/^{238}U$ ages for rim domains.

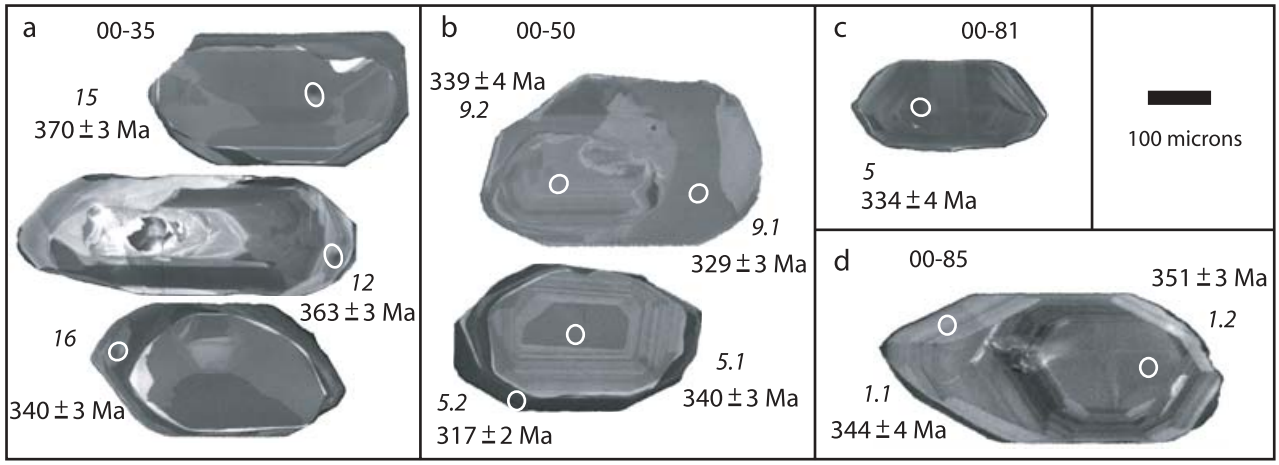

Figure 8. Cathodoluminescence (CL) images of representative zircon grains from dated pegmatites showing locations of SHRIMP analysis pits, grain number, spot number, and corresponding U–Pb age (± 1σ Ma). Scale is the same for all images. (a) Core (spot 15), intermediate rim (spot 12), and high U rim (spot 16) domains in sample 00-35. (b) Core (spots 5.1 and 9.2), intermediate rim (spot 9.1), and high U rim (spot 5.2) domains in sample 00-50. (c) Homogeneous zircon in sample 00-81. (d) Zircon showing slight U and age variation between core (spot 1.2) and rim (spot 1.1) domains overgrown by very thin higher U rim in sample 00-85. An age distinction between core and rim domains for this sample was not resolved during this study.

low-strain, dilational structural setting. This is consistent with the observation that the pegmatites, although generally not deformed, are compositionally and texturally heterogeneous at the outcrop scale. The oldest age obtained for sample 00-35 is interpreted as a minimum age for boudin development in the Danmarkshavn area.

5. Discussion

The growing geochronological database for the North-East Greenland eclogite province suggests that the formation and exhumation of eclogitic rocks in the Greenland Caledonides is generally younger and more protracted than previously documented, with HP metamorphism occurring in the central block between 410 and 390 Ma and UHP metamorphism at 360 Ma (Gilotti, Nutman & Brueckner, 2004). Relationships in the Danmarkshavn area define the protracted retrograde metamorphic and deformational history of the central block. Pegmatite emplacement into strain shadows between mafic boudins indicates that retrogression and deformation were ongoing by 375 Ma. Deformation during retrograde metamorphism included reactivation of the metamorphic foliation, formation of widely distributed discrete dextral shear zones, and presumably continued displacement along the Germania Land deformation zone into sub-amphibolite facies conditions. A dextral component to early bulk shear within the gneisses is suggested by the sigmoidal shape of some mafic pods (Fig. 5c) and ubiquitous right-lateral kinematic indicators within the gneisses. Following the early boudinage and pegmatite emplacement, dextral deformation became localized into discrete shear zones in the Danmarkshavn area. The ductile component of the dextral deformation locally ended by 340 Ma, the age of the oldest cross-cutting pegmatite. Biotite and hornblende grew in shear bands in the mylonites under amphibolite facies conditions. Biotite cooling ages recorded by Rb–Sr mineral isochrons from a Danmarkshavn garnet websterite and a banded amphibolitic gneiss are 326 ± 6 Ma (Brueckner, Gilotti & Nutman, 1998) and 321 ± 10 Ma (Steiger *et al.* 1976), respectively, suggesting a prolonged cooling history. Partial replacement of biotite by chlorite in some of the mylonites indicates continued deformation at greenschist facies conditions.

Localization of deformation at Danmarkshavn was presumably contemporaneous with the beginning of strain localization in the Germania Land deformation zone. The widespread discrete mylonite zones in the Danmarkshavn area are geometrically and kinematically identical to the Germania Land deformation zone, suggesting that the structures are part of the same family of deformation zones. While the amphibolite facies dextral shear zones at Danmarkshavn were becoming inactive by 340 Ma, strain continued to be localized at shallower levels along the Germania Land deformation zone well into greenschist facies (Hull & Gilotti, 1994), overprinting its initial amphibolite facies metamorphic assemblage.

The timing relationships established here suggest that the dextral shear zones, and by inference the Germania Land deformation zone, may have played an important role in the exhumation of the HP/UHP rocks along the eastern margin of the North-East Greenland eclogite province. Strike-slip deformation along the Germania Land deformation zone was coeval with formation of UHP rocks in the eastern block at about 360 Ma (Gilotti, Nutman & Brueckner, 2004). Steeply plunging lineations occur in some of the eclogites, gneisses and mylonites, suggesting that vertical stretching started in the final stage of eclogite facies metamorphism and continued during amphibolite facies

retrogression at the same time as the dextral shearing. Thus it appears that the area deformed under a transpressional regime, and that the gneisses experienced triclinic shear (Fossen & Tikoff, 1998; Lin, Jiang & Williams, 1998; Jiang, Lin & Williams, 2001; Williams & Vernon, 2001) and some degree of vertical extrusion (Thompson, Schulmann & Jezek, 1997*a*, *b*). Vertical extrusion along the mylonitic Germania Land deformation zone would have accommodated the initial stages of exhumation and transition from eclogite to amphibolite facies conditions in the central block followed by exhumation of the eastern block.

After the first stage of exhumation along deep structures (that is, the Germania Land deformation zone) between 370 and *c.* 340 Ma, a second stage of exhumation of the HP rocks would have been accommodated at shallower crustal levels by continued displacement along the Germania Land deformation zone at greenschist facies and lower conditions. The brittle Chatham Elv fault could be responsible for late-stage exhumation because of its age and the presence of a dip-slip component. Displacement on the Chatham Elv fault has not been directly dated, however, late Carboniferous sediments are juxtaposed against basement gneisses to the east of the fault (Piasecki *et al.* 1994). Hull & Gilotti (1994) suggest that faulting and sedimentation were concurrent, based on spatial relationships between sedimentary facies and fault geometry. Tilting of the sediments away from the fault suggests that the movement along the fault had a dip-slip component (Hull & Gilotti, 1994).

A late Carboniferous age for this proposed second pulse of exhumation is consistent with the widespread extension that took place in the Carboniferous all over the North Atlantic–Arctic region (Larsen, 1990; Stemmerik & Piasecki, 1990; Stemmerik, Vigran & Piasecki, 1991). Shallow shelf environments started to form in the Finnmark Platform region in the late Visean, and open marine environments, offshore of present North and North-East Greenland, developed in the Moscovian (Stemmerik, 2000; Stemmerik & Worsley, 2005). Evidence of late Carboniferous extension is also present in North Greenland as faulting along the Harder Fjord Fault Zone and rifting on Svalbard (Piepjohn & von Gosen, 2001), and further south in East Greenland as faulting along the southern extension of the Storstrømmen shear zone (Vigran, Stemmerik & Piasecki, 1999).

6. Conclusions

The data presented in this paper lead to the following conclusions:

(1) Based on the ages of boudin neck pegmatites at Danmarkshavn that are consistent with regional titanite geochronology, we conclude that initial exhumation and retrograde metamorphism of the central and western blocks were ongoing by 370 Ma.

(2) By 370 Ma, the gneisses at Danmarkshavn were ductilely deformed by bulk shear with a dextral component during exhumation of the central block.

(3) Between 370 Ma and 340 Ma, the dextral deformation became concentrated into discrete mylonitic shear zones while the area was still experiencing amphibolite facies conditions.

(4) The Danmarkshavn mylonite zones became inactive during greenschist facies conditions, when most of the greenschist facies displacement became restricted to the Germania Land deformation zone after 340 Ma.

(5) The strain localization into narrow deformation zones is inferred to record the continued exhumation and cooling of the central block primarily during the Carboniferous.

(6) Coesite-bearing eclogites of the eastern block might have been exhumed from UHP to amphibolite facies conditions after 360 Ma by displacement along the Germania Land deformation zone in a transpressional setting. Final exhumation most likely occurred via steep, brittle normal faults, such as the Chatam Elv fault, concurrent with Carboniferous basin development.

(7) Future geochronological studies of pegmatites possibly associated with the Germania Land deformation zone and the Chatam Elv fault are needed to test the regional applicability of our interpretation.

Acknowledgements. The National Geographic Society (Grant 6853-00 to Gilotti) provided funding for the fieldwork. Additional support came from National Science Foundation grants EAR-0208236 and EAR-0208158 awarded to Gilotti and McClelland, respectively. The Graduate College at the University of Iowa provided partial funding to Sartini-Rideout to present this material at the Alice Wain Memorial West Norway Eclogite Field Symposium. We thank Matt Burreson and Alan Pedersen for their cheerful assistance in the field, and the staff at the Danmarkshavn Weather Station for their wonderful hospitality during our work. Stereonets were plotted using version 2.45 of StereoNett. Discussions with Joe Wooden and C. T. Foster Jr, and reviews by Clark Friend and Lars Stemmerik, improved the manuscript.

References

ANDERSEN, T. B., JAMTVEIT, B., DEWEY, J. F. & SWENSSON, E. 1991. Subduction and eduction of continental crust: major mechanisms during continent–continent collision and orogenic extensional collapse, a model based on the south Norwegian Caledonides. *Terra Nova* **3**, 303–10.

AVÉ LALLEMANT, G. H. 1996. Displacement partitioning of arc-parallel extension; example from the south-eastern Caribbean–South-American plate interaction. *Geophysical Monograph* **96**, 113–18.

BARTH, A. P., WOODEN, J. L. & COLEMAN, D. S. 2001. SHRIMP-RG U–Pb zircon geochronology of Mesoproterozoic metamorphism and plutonism in the southwestern United States. *Journal of Geology* **109**, 319–27.

BEAUMONT, C., FULLSACK, P. & HAMILTON, J. 1994. Styles of crustal deformation in compressional orogens caused by subduction of the underlying lithosphere. *Tectonophysics* **232**, 119–32.

BREY, G. P. & KOHLER, T. 1990. Geothermobarometry in four-phase lherzolite. II. New thermobarometers, and practical assessment of existing thermobarometers; experimental results from 10 to 60 kb. *Journal of Petrology* **31**, 1353–78.

BRONNER, F. E. 1948. Contributions to the geology. In *The coast of North-East Greenland* (ed. L. A. Boyd), pp. 211–24. American Geographical Society, Special Publication no. 30.

BRUECKNER, H. K., GILOTTI, J. A. & NUTMAN, A. P. 1998. Caledonian eclogite-facies metamorphism of early Proterozoic protoliths from the North-East Greenland Eclogite Province. *Contributions to Mineralogy and Petrology* **130**, 103–20.

CHADWICK, B. & FRIEND, C. R. L. 1994. Reaction of Precambrian high-grade gneisses to mid-crustal ductile deformation in western Dove Bugt, North-East Greenland. *Rapport Grønlands Geologiske Undersøgelse* **162**, 53–70.

CHEMENDA, A. I., MATTAUER, M. & BOKUN, A. N. 1996. Continental subduction and a mechanism for exhumation of high-pressure metamorphic rocks: new modeling and field data from Oman. *Earth and Planetary Science Letters* **143**, 173–82.

CHEMENDA, A. I., MATTAUER, M., MALAVIEILLE, J. & BOKUN, A. N. 1995. A mechanism for syn-collisional deep rock exhumation and associated normal faulting: results from physical modeling. *Earth and Planetary Science Letters* **132**, 225–32.

CHOPIN, C. 2003. Ultrahigh-pressure metamorphism: tracing continental crust into the mantle. *Earth and Planetary Science Letters* **212**, 1–14.

DEUTMEYER, K. J., DORSCH, S., SARTINI-RIDEOUT, C., GILOTTI, J. A. & WULFF, A. H. 2001. Using geochemistry to discern the protoliths of layered eclogites and dykes from the Danmarkshavn area, North-East Greenland Caledonides. *Geological Society of America Abstracts with Programs* **33**(4), 50.

DEWEY, J. F. 1988. Extensional collapse of orogens. *Tectonics* **7**, 1123–39.

DEWEY, J. F. & STRACHAN, R. A. 2003. Changing Silurian–Devonian relative plate motion in the Caledonides: sinistral transpression to sinistral transtension. *Journal of the Geological Society, London* **160**, 219–29.

ELVEVOLD, S. & GILOTTI, J. A. 2000. Pressure–temperature evolution of retrogressed kyanite-eclogites, Weinschenk Island, North-East Greenland Caledonides. *Lithos* **53**, 127–47.

ERNST, W. G. & LIOU, J. G. 2000. Overview of UHP metamorphism in well studied collisional orogens. In *Ultrahigh-pressure metamorphism in collision type orogenic belts* (eds W. G. Ernst and J. G. Liou), pp. 3–19. Columbia, Maryland: Bellwether Publishing.

FOSSEN, H. & TIKOFF, B. 1998. Extended models of transpression and transtension, and application to tectonic settings. In *Continental Transpressional and Transtensional Tectonics* (eds R. E. Holdsworth, R. A. Strachan and J. F. Dewey), pp. 15–33. Geological Society of London, Special Publication no. 135.

GILOTTI, J. A. 1993. Discovery of a medium-temperature eclogite province in the Caledonides of North-East Greenland. *Geology* **21**, 523–6.

GILOTTI, J. A. 1994. Eclogites and related high-pressure rocks from North-East Greenland. *Rapport Grønlands Geologiske Undersøgelse* **162**, 77–90.

GILOTTI, J. A., NUTMAN, A. P. & BRUECKNER, H. K. 2004. Devonian to Carboniferous collision in the Greenland Caledonides: U–Pb zircon and Sm–Nd ages of high-pressure and ultrahigh-pressure metamorphism. *Contributions to Mineralogy and Petrology* **148**, 216–35.

GILOTTI, J. A. & RAVNA, E. J. K. 2002. First evidence for ultrahigh-pressure metamorphism in the North-East Greenland Caledonides. *Geology* **30**, 551–4.

HALLETT, B. W., MCCLELLAND, W. C., GILOTTI, J. A., POWER, S. E. & TUCKER, R. D. 2005. Timing of displacement on the Storstrømmen Shear Zone, North-East Greenland Caledonides. *Geological Association of Canada – Mineralogical Association of Canada Abstracts with Programs* **30**, 78.

HENRIKSEN, N. 1997. *Geological Map of Greenland, 1:500 000, Dove Bugt, Sheet 10*. Copenhagen: Geological Survey of Denmark and Greenland.

HENRIKSEN, N. 2003. *Caledonian Orogen, East Greenland 70°–82°N. Geologic map 1:1 000 000*. Copenhagen: Geological Survey of Denmark and Greenland.

HOLDSWORTH, R. E. & STRACHAN, R. A. 1991. Interlinked system of ductile strike-slip and thrusting formed by Caledonian sinistral transpression in northeastern Greenland. *Geology* **19**, 1510–13.

HULL, J. M., FRIDERICHSEN, J. D., GILOTTI, J. A., HENRIKSEN, N., HIGGINS, A. K. & KALSBEEK, F. 1994. Gneiss complex of the Skaerfjorden region (76°–78° N), North-East Greenland. *Rapport Grønlands Geologiske Undersøgelse* **162**, 35–51.

HULL, J. M. & GILOTTI, J. A. 1994. The Germania Land deformation zone, North-East Greenland. *Rapport Grønlands Geologiske Undersøgelse* **162**, 113–27.

HULL, J. M., GILOTTI, J. A. & FRIDERICHSEN, J. D. 1995. A window through a basement-involved thrust sheet into sub-thrust cover, north-east sector, East Greenland Caledonides. *Geological Society of America Abstracts with Programs* **27**(6), 225.

JEPSEN, H. F. 2000. *Geological Map of Greenland, 1:500,000, Lambert Land, Sheet 9*. Copenhagen: Geological Survey of Demark and Greenland.

JIANG, D., LIN, S. & WILLIAMS, P. F. 2001. Deformation path in high-strain zones, with reference to slip partitioning in transpressional plate-boundary regions. *Journal of Structural Geology* **23**, 991–1005.

KALSBEEK, F. 1995. Geochemistry, tectonic setting, and poly-orogenic history of Palaeoproterozoic basement rocks from the Caledonian fold belt of the North-East Greenland. *Precambrian Research* **72**, 301–15.

KALSBEEK, F., NUTMAN, A. P. & TAYLOR, P. N. 1993. Palaeoproterozoic basement province in the Caledonian fold belt of North-East Greenland. *Precambrian Reasearch* **63**, 163–78.

KRABBENDAM, M. & DEWEY, J. F. 1998. Exhumation of UHP rocks in the Western Gneiss region, Scandinavian Caledonides. In *Continental transpressional and transtensional tectonics* (eds R. E. Holdsworth, R. A. Strachan and J. F. Dewey), pp. 159–81. Geological Society of London, Special Publication no. 135.

LARSEN, H. C. 1990. The East Greenland Shelf. In *The Arctic Ocean Region, The Geology of North America* (eds A. Grantz, L. Johnson and J. F. Sweeny),

pp. 185–210. Geological Society of America, Boulder, Colorado.

LIN, S., JIANG, D. & WILLIAMS, P. F. 1998. Transpression (or transtension) zones of triclinic symmetry: natural example and theoretical modeling. In *Continental transpressional and transtensional tectonics* (eds R. E. Holdsworth, R. A. Strachan and J. F. Dewey), pp. 41–57. Geological Society of London, Special Publication no. 135.

LUDWIG, K. R. 1999. Isoplot/EX version 2.10: a geochronological toolkit for Microsoft Excel. *Berkeley Geochronology Center Special Publication* **1**, 1–49.

LUDWIG, K. R. 2001. Squid version 1.02: A users manual. *Berkeley Geochronology Center Special Publication* **2**, 1–22.

MANN, P. & GORDON, M. B. 1996. Tectonic uplift and exhumation of blue-schist basalts along transpressional strike-slip fault zones. *Geophysical Monograph* **96**, 143–54.

MASSONE, H. T. & O'BRIEN, P. J. 2003. The Bohemian Massif and the NW Himalaya. In *Ultrahigh-pressure Metamorphism* (eds D. A. Carswell and R. Compagnoni), pp. 145–87. European Mineralogical Union Notes in Mineralogy 5.

MCCLELLAND, W. C. & GILOTTI, J. A. 2003. Bracketing the age of HP metamorphism in the Greenland Caledonides: New U–Pb SHRIMP-RG age determinations on retrograde amphibolite facies metamorphism. The Alice Wain Memorial West Norway Eclogite Field Symposium. *Norges Geologiske Undersøgelse Report* **2003.055**, 97–8.

MCCLELLAND, W. C., GILOTTI, J. A., POWER, S. E. & MAZDAB, F. K. 2005. Dating of UHP metamorphism, NE Greenland Caledonides. *Mitteilungen der Österreichischen Mineralogischen Gesellschaft* **150**, 107.

NUTMAN, A. P. & KALSBEEK, F. 1994. Search for Archaean basement in the Caledonian fold belt of North-East Greenland. *Rapport Grønlands Geologiske Undersøgelse* **162**, 129–33.

PASSCHIER, C. W. 2001. Flanking structures. *Journal of Structural Geology* **23**, 951–62.

PIASECKI, S., STEMMERIK, L., FRIDERICHSEN, J. D. & HIGGINS, A. K. 1994. Stratigraphy of the post-Caledonian sediments in the Germania Land area, North-East Greenland. *Rapport Grønlands Geologiske Undersøgelse* **162**, 177–84.

PIAZOLO, S. & PASSCHIER, C. W. 2002. Controls on lineation development in low to medium grade shear zones: a study from the Cap de Creus peninsula, NE Spain. *Journal of Structural Geology* **24**, 25–44.

PIEPJOHN, K. & VON GOSEN, W. 2001. Polyphase deformation at the Harder Fjord Fault Zone (North Greenland). *Geological Magazine* **138**, 407–34.

PLATT, J. P. 1986. Dynamics of orogenic wedges and the uplift of high-pressure metamorphic rocks. *Geological Society of America Bulletin* **97**, 1037–53.

POWER, S. E., GILOTTI, J. A., MCCLELLAND, W. C. & WOPENKA, B. 2004. Laser Raman Microprobe identification of coesite in kyanite eclogites and their host gneisses, North-East Greenland Caledonides. *Geological Society of America Abstracts with Programs* **36**(5), 453.

SHATSKY, V. S. & SOBOLEV, N. V. 2003. The Kochetav massif of Kazakstan. In *Ultrahigh-pressure Metamorphism* (eds D. A. Carswell and R. Compagnoni), pp. 75–103. European Mineralogical Union Notes in Mineralogy 5.

STEIGER, R. H., HARNIK-SOPTRAJANOVA, G., ZIMMERMANN, E. & HENRIKSEN, N. 1976. Isotopic age and metamorphic history of the banded gneisses at Danmarkshavn, East Greenland. *Contributions to Mineralogy and Petrology* **57**, 1–24.

STEMMERIK, L. 2000. Late Paleozoic evolution of the North Atlantic margin of Pangea. *Paleogeography, Paleoclimatology, Paleoecology* **161**, 95–126.

STEMMERIK, L. & PIASECKI, S. 1990. Post-Caledonian sediments in North-East Greenland between 76° and 78°30′ N. *Rapport Grønlands Geologiske Undersøgelse* **148**, 123–6.

STEMMERIK, L., VIGRAN, J. O. & PIASEKI, S. 1991. Dating of late Paleozoic rifting events in the North-Atlantic: New biostratigraphic data from the uppermost Devonian and Carboniferous of East Greenland. *Geology* **19**, 218–21.

STEMMERIK, L. & WORSLEY, D. 2005. 30 years on – Arctic Upper Palaeozoic stratigraphy, depositional evolution and petroleum prospectivity. *Norwegian Journal of Geology* **85**, 151–68.

STIPP, M., STUNITZ, H., HEILBRONNER, R. & SCHMIDT, S. M. 2002. The eastern Tonale fault zone: a 'natural laboratory' for crystal plastic deformation of quartz over a temperature range from 250 to 700°C. *Journal of Structural Geology* **24**, 1861–84.

STRACHAN, R. A. & TRIBE, I. R. 1994. Structure of the Storstrømmen shear zone, eastern Hertugen af Orleans Land, North-East Greenland. *Rapport Grønlands Geologiske Undersøgelse* **148**, 123–6.

THOMPSON, A. B., SCHULMANN, K. & JEZEK, J. 1997*a*. Extrusion tectonics and elevation of lower crustal metamorphic rocks in convergent orogens. *Geology* **25**, 491–4.

THOMPSON, A. B., SCHULMANN, K. & JEZEK, J. 1997*b*. Thermal evolution and exhumation in obliquely convergent (transpressive) orogens. *Tectonophysics* **280**, 171–84.

TULLIS, J. & YUND, R. A. 1985. Dynamic recrystallization of feldspar: a mechanism for ductile shear zone formation. *Geology* **13**, 238–41.

TULLIS, J. & YUND, R. A. 1991. Diffusion creep in feldspar aggregates: experimental evidence. *Journal of Structural Geology* **13**, 987–1000.

VIDAL, J. L., KUBIN, L., DEBAT, P. & SOULA, J. L. 1980. Deformation and dynamic recrystallization of K-feldspar augen in orthogneiss from Montagne Noir, Occitania. *Lithos* **13**, 247–57.

VIGRAN, J. O., STEMMERIK, L. & PIASECKI, S. 1999. Stratigraphic and depositional evolution of the uppermost Devonian–Carboniferous (Tournaisian–Westphalian) non-marine deposits in North-east Greenland. *Palynology* **23**, 115–52.

WILLIAMS, I. S. 1997. U–Pb by ion microprobe. In *Applications of microanalytical techniques to understanding mineralizing processes* (eds M. A. McKibben, W. C. Shanks and W. I. Ridley), pp. 1–35. Society of Economic Geologists, Reviews in Economic Geology 7.

WILLIAMS, P. F. & VERNON, R. H. 2001. Origin of a vertical lineation in conjugate transcurrent shear-zones at Broken Hill, Australia. *Tectonophysics* **335**, 163–82.

WYLLIE, P. J. 1957. A geological reconnaissance through South Germania Land, Northeast Greenland, lat. 77°N, long. 18°W to 22°W. *Meddeleser om Grønland* **157**(1), 66 pp.